ChemPubSoc Europe

DOI: 10.1002/open.201500136

Open Access ChemistryOPEN Full Papers

Structural Preferences in Phosphanylthiolato Platinum(II) Complexes

Josep Duran,[a] Alfonso Polo,*[a] Julio Real,[b] Jordi Benet-Buchholz,[c] Miquel Solà,[a, d] and Albert Poater*[a, d]

The transition-metal complexes of heterotopic phosphanylthiolato ligands are useful in various reactions which depend on the stereochemistry of the complexes. Bis-chelate complex [Pt($SCH_2CH_2PPh_2$-κ^2P,S)$_2$] (**1**) was obtained in good yields by direct base-free substitution reaction of the corresponding phosphanylthiol ($HSCH_2CH_2PPh_2$) with K_2PtCl_4 or by oxidative addition of the same phosphanylthiol to $Pt(PPh_3)_4$. In agreement with the antisymbiosis rule, complex **1** shows a *cis*-P,P arrangement in solid state crystallizing in the monoclinic system (*C2/c*). Density functional theory (DFT) calculations on **1** reveal the right characteristics for the preferred *cis*-P,P arrangement, rationalizing its formation. Direct base-free reaction of [$PtCl_2$(1,5-cyclooctadiene)] with one equivalent of the same phosphanylthiol produce the trinuclear complex [PtCl(μ-$SCH_2CH_2PPh_2$-κ^2P,S)]$_3$ (**2**) instead of the binuclear structure common in palladium and nickel derivatives. Crystals of **2** are triclinic ($P\bar{1}$) showing a sulfur-bridging edge-sharing cyclic trinuclear complex with square-planar coordination geometry around the platinum atoms and a Pt_3S_3 cycle in skew-boat conformation. This preference for the trinuclear structure was rationalized mechanistically and through conceptual DFT.

Introduction

The transition-metal complexes of heterotopic phosphanylthiolato ligands have been widely studied because of their applicability in some interesting reactions,[1] such as S-alkylation/S-dealkylations,[2,3] carbothiolations,[3] reductions,[4] copolymerizations,[5] or carbonylations.[6] These complexes also have relevance in desulfurization technologies[7] and in understanding the biological pathways of certain sulfur-containing metalloproteins.[8] For all these applications, the stereochemistry of these complexes has particular importance, as different stereoisomers could present different behavior in a given process.[9] Among all phosphanylthiolato ligands, we are particularly interested in 2-phosphanylalkylthiolato ligands because they can support a resolved chiral carbon in the chelate chain.[10,11] For group 10 metals (M=Ni, Pd, and Pt), the more abundant 2-phosphanylalkylthiolato complexes are the bis-chelates, [M(ligand-κ^2P,S)$_2$], and the chlorocomplexes, [MCl(μ$_S$-ligand-κ^2P,S)]$_2$ or [MCl(ligand-κ^2P,S)(PR_3)].

Taking as a model the 2-(diphenylphosphanyl)ethanethiol (Hdppet) derivatives, [Ni(dppet)$_2$] shows a *trans*-P,P arrangement, both in solution and in the solid state.[12] The same preferred stereochemistry was proposed for other nickel bis-chelates.[10c,12,13] For [Pd(dppet)$_2$], a *trans*-P,P geometry in solution was proposed by comparison with the bis[2-(dimethylphosphanyl)ethanethiolato] complex which shows characteristic virtual couplings for the methyl groups in the ^{1}H and ^{13}C{^{1}H} NMR spectra.[14] The solid-state structure of [Pd(dppet)$_2$] is unknown, but a *trans*-P,P arrangement is supported by the stereochemistry observed in other bis-chelates with chain-substituted ligands.[10a–b,11a] Contrasting with [Pd(dppet)$_2$], some of these complexes show an equilibrium between the two geometric isomers (*cis/trans*) in solution.[10a,11a,13] Also the crystal structure of [Pt(dppet)$_2$] (**1**) is unknown, and both *cis*[11a] and *trans*[10b] geometries in solid state were observed for other platinum bis[phosphanylalkylthiolato] complexes. In solution, a *cis*-P,P stereochemistry was suggested for **1** because of the absence of NMR virtual couplings in some platinum bis[(2-methylphosphanyl)ethanethiolato] analogues,[13,14] and by the large value of the $^1J_{P-Pt}$ coupling constant.[14] However, as we showed previously, the $^1J_{P-Pt}$ criterion is not always infallible.[10b] In keeping

[a] Dr. J. Duran, Dr. A. Polo, Prof. Dr. M. Solà, Dr. A. Poater
Departament de Química, Universitat de Girona
Campus de Montilivi s/n, 17071 Girona (Spain)
E-mail: alfons.polo@udg.edu

[b] Dr. J. Real
Departament de Química, Universitat Autònoma de Barcelona
08193 Bellaterra (Spain)

[c] Dr. J. Benet-Buchholz
Institute of Chemical Research of Catalonia (ICIQ)
Av. Països Catalans 16, 43007 Tarragona (Spain)

[d] Prof. Dr. M. Solà, Dr. A. Poater
Institut de Química Computational i Catàlisi, Universitat de Girona
Campus de Montilivi s/n, 17071 Girona (Spain)
E-mail: albert.poater@udg.edu

Supporting information and ORCID(s) from the author(s) for this article are available on the WWW under http://dx.doi.org/10.1002/open.201500136. Data include Cartesian xyz coordinates and energies of all optimized reactants, products, intermediates, and transition states. CCDC 1401716 and 1401717 contain the supplementary crystallographic data for this paper. These data are provided free of charge by The Cambridge Crystallographic Data Centre.

with the chlorocomplexes, nickel has preference for the binuclear complex [NiCl(μ-$SCH_2CH_2PPh_2$-κ^2*P,S*)]$_2$,[15] also observed for other phosphanylalkylthiolato ligands, both in solution and in solid state.[10c, 11a] Mononuclear [PdCl(dppet-κ^2*P,S*)(PPh_3)] proved to be stable in solution. No loss of PPh_3 takes place, and no dimeric palladium complexes were ever detected.[6] This complex shows in solution an equilibrium between the two geometric isomers strongly displaced to the *trans*-P,P arrangement, but crystallization yields only the major stereoisomer. When an alkyl substituent is introduced in the chelate chain, as in the case of 1-(diphenylphosphanyl)butyl-2-thiolato derivative, dissociation of PPh_3 and formation of the dimeric chlorocomplex, [PdCl(μ$_S$-ligand-κ^2*P,S*)]$_2$, was described.[11a] For platinum, only the mononuclear *cis*-[PtCl(dppet-κ^2*P,S*)(PPh_3)] was reported.[16]

As part of a project on the analysis of the ligand-based stereoelectronic effects that are determinant in the coordination conformations of phosphanylthiolato ligands around the metal,[6, 10–12] we now report new preparation methods, and the solid state structure, for bis-chelate **1** and for the unusual trinuclear complex [PtCl(μ-$SCH_2CH_2PPh_2$-κ^2*P,S*)]$_3$ (**2**). The structures obtained are also rationalized mechanistically and through conceptual DFT calculations.

Results and Discussion

Complex **1** was first prepared in moderate yield (52%) from the reaction of K_2PtCl_4 and Hdppet in the presence of NEt_3 as a base.[14] The potential problems related to the use of the base,[10a] together with the low yield of **1** with this method, prompted us to explore the direct, base-free, procedure. Thus, reaction of K_2PtCl_4 with 2 equivalents of Hdppet in a mixture of methanol/water cleanly afforded bis-chelate **1**, which was isolated in 92% yield (Scheme 1). Alternatively, **1** can be also

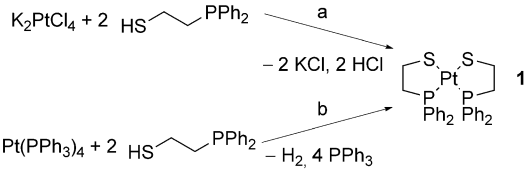

Scheme 1. Synthesis of bis-chelate **1**. *Reagents and conditions*: a) Hdppet/MeOH, K_2PtCl_4/H_2O, 30 min, rt, 92%; b) Hdppet (neat), $Pt(PPh_3)_4/CH_2Cl_2$, 30 min, rt, 70%.

obtained by oxidative addition of the phosphanylthiol to $Pt(PPh_3)_4$ and subsequent reductive elimination of hydrogen. In this case, bis-chelate **1** was isolated in 70% yield (Scheme 1). According to the $^{31}P\{^1H\}$ NMR spectrum, bis-chelate **1** exists as a single geometric isomer in solution, with a $^1J_{P-Pt}$ coupling constant of 2810.9 Hz which suggest a *cis*-P,P arrangement.[14] The *cis* geometry of bis-chelate **1** in solid state was confirmed by the X-ray diffraction (XRD) crystal structure.

The XRD study was carried out on a crystal of **1** obtained from dichloromethane–hexane. Crystal data for the structure are given in Table 1. Selected bond lengths and bond angles are listed in the caption of Figure 1. The crystal structure reveals a mononuclear square-planar complex with C_2 symmetry and the platinum atom placed on the rotation axis (Figure 1).

Table 1. Crystal data for **1** and **2**

Compound	**1**	**2**
Formula	$C_{28}H_{28}P_2Pt_1S_2$	$C_{42}H_{42}Cl_3P_3Pt_3S_3$
Solvents	–	–
Formula weight	685.65	1427.47
Crystal size (mm^3)	0.30×0.20×0.10	0.003×0.003×0.002
Crystal color	yellow	yellow
Temp (K)	153	153
Crystal system	monoclinic	triclinic
Space group	*C*2/*c*	*P*$\bar{1}$
A (Å)	14.6509(3)	12.2393(5)
B (Å)	10.7332(2)	13.4900(6)
C (Å)	17.0890(3)	15.4706(7)
α (deg)	90	113.7590(10)
β (deg)	109.3020(10)	105.505(2)
γ (deg)	90	95.164(2)
V (Å^3)	2536.21(8)	2195.42(17)
Z	4	2
ρ (g cm^{-}3)	1.796	2.159
μ (mm^{-1})	5.839	10.000
θ_{max} (°)	31.52	31.53
Reflec. measured	19126	30667
Unique reflections	3948 [R_{int} = 0.0593]	8180 [R_{int} = 0.0821]
Absorpt. correct.	SADABS	SADABS
Trans. min/max	0.587/1.000	0.506/1.000
Parameters/restraints	206	647/834
R1/wR2 [$I > 2\sigma(I)$]	0.0295/0.0709	0.0458/0.0908
R1/wR2 [all data]	0.0304/0.0716	0.0910/0.1008
Goodness-of-fit (F^2)	1.052	0.857
Peak/hole (e/Å^3)	1.993/−5.137	2.056/−3.358

The Pt–S bond length is similar to those detected in other *cis*-[16] and *trans*-bis(phosphanylthiolato)[15] complexes of platinum(II), but the Pt–P is shorter than those observed in the *trans* geometries. The large P–Pt–P angle, nearly 105°, results from the *cis* orientation of the bulky PPh_2 groups that compress the S–Pt–S angle to about 82°. The chelate angle, is in the order of those observed for mononuclear platinum(II) com-

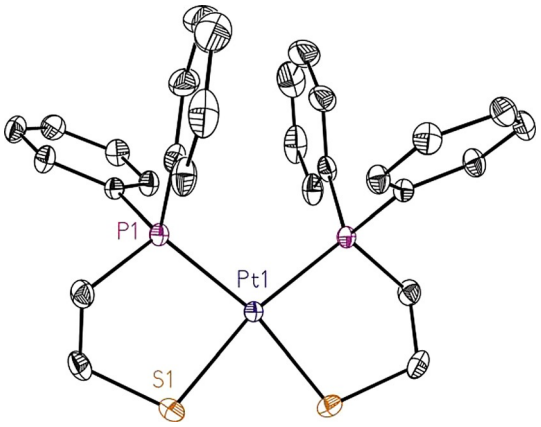

Figure 1. ORTEP (Oak Ridge Thermal Ellipsoid Plot) figure (50%) of complex **1**, H atoms are omitted for the sake of clarity; selected distances (Å) and angles (°): Pt–P 2.2705(6), Pt–S 2.3233(6), P–Pt–S 86.45(2), P–Pt–P^i 104.98(3), S–Pt–S^i 82.14(3), P–Pt–S^i 168.56(2). Symmetry transformation used to generate equivalent atoms: -x, y, $^1/_2$-z.

plexes with the PPh_2 group of a chelated dppet ligand *cis* to a PPh_3.[16]

The observed structural *cis* preference can be interpreted, in simple terms, on the basis of the antisymbiosis rule stating that two soft ligands in mutual *trans* positions have a destabilizing effect on each other when attached to a soft metal ion.[17] To shed light into this preference for the *cis* conformation and get more detailed information, we envisaged density functional theory (DFT) calculations. For our study, we used the M06 exchange-correlation functional that includes dispersion corrections. M06/TZVP//M06/SVP calculations on complex **1** reveal a favorable energy difference of only 1.3 kcal mol^{-1} for the *cis* isomer. This small difference can be the result of a low antisymbiotic effect (thiolates and phosphines are both soft bases; for example, hardness of CH_3S^- and PPh_2CH_3 are 61.8 and 65.9 kcal mol^{-1}, respectively) and the steric interactions that favor the *trans* isomer. When the thermal and entropic effects are not introduced, the energetic preference for the *cis* arrangement increases to 3.7 kcal mol^{-1}, which brings the computational results into much better agreement with experimental observations, and reveals a possible overestimation by our calculations of the entropic stabilization of the *trans* isomer as compared to the *cis* one. The large dipole moment of the *cis* isomer provides larger solvation energy in comparison with the nonpolar *trans* isomer.[18] The chemical potential for the *cis* isomer of complex **1** is −70.5 kcal mol^{-1} whereas it is −66.2 kcal mol^{-1} for the *trans* conformation.[19] In agreement with the maximum hardness principle,[20] the chemical hardness of the *cis* conformation (41.5 kcal mol^{-1}) is somewhat higher than that of the *trans* conformation (41.3 kcal mol^{-1}).[21]

Given the low energy difference between both isomers, we investigated the reaction pathway to get complex **1** from $Pt(PPh_3)_4$ (see Figure 2) in the *cis* and *trans* conformations to discern whether kinetic effects are responsible for the formation of exclusively the *cis* isomer. Formation of the *cis* isomer requires the generation of complex **V** in Figure 2. These complexes are generated by successive substitutions of phosphine by Hdppet ligands. The sequential dissociation of phosphine groups is not energy demanding, provided that at least two based phosphorous ligands remain bonded to platinum, either in the form of triphenylphosphines or phosphanylthiol ligands. Indeed the bis-phosphine structure is isoenergetic with the bis-Hdppet structure (compare complexes **III** and **VII**). This result concurs with the experimental fact that in the presence of a high concentration of Hdppet with respect to the $Pt(PPh_3)_4$ precursor, the PPh_3 groups are easily substituted. In any case the coordination of the phosphanylthiolato does not occur through the thiolate moiety, but through the phosphine group. Take for instance the coordination of the second molecule of Hdppet to species **VIII**, from which formation of complex **X** with the phosphine coordinated to Pt is 20.0 kcal mol^{-1} more stable than the same complex coordinated through the thiol group. Once complex **V** is formed, the next dissociation of a phosphine ligand is not feasible without the oxidative addition of the S–H bond of the Hdppet ligand into the Pt center to form complex **IX**. Actually without removing the phosphine ligand, from complex **V**, this insertion takes places through a barrier of 11.5 kcal mol^{-1}. From **IX**, bearing the excess of Hdppet, the exchange of PPh_3 by Hdppet is favored by 1.6 kcal mol^{-1}, to form complex **X**. The final step that leads to complex ***1 cis*** from species **X** takes places through a concerted transition state that involves a second oxidative addition and the reductive release of a hydrogen molecule in a process that requires 25.9 kcal mol^{-1}. This rather high energy barrier is probably somewhat overestimated. The rate determining step (rds) for the formation of ***1 cis*** corresponds to this last **X** to ***1 cis*** transformation.

The *trans* conformation of complex **1** can be formed through different reaction pathways. First, it might be generated directly from the *cis* conformation, that is, complex ***1 cis***,

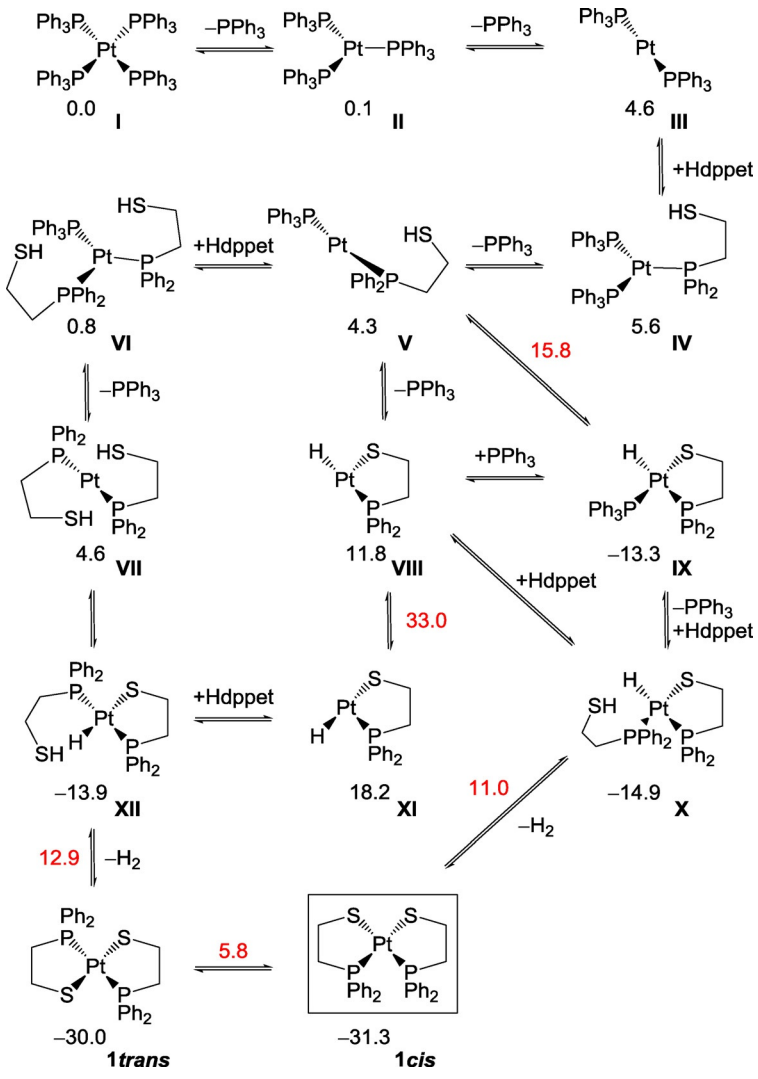

Figure 2. Reaction pathways of the conversion of $Pt(PPh_3)_4$ to complex **1** (red: the values of the transition states, relative Gibbs energies in kcal mol^{-1}).

however the barrier to isomerize to the *trans* conformation is 37.1 kcal mol^{-1}. Second, complex **V** can also evolve to **VII** through successive exchange of phosphines by Hdppet ligands. Two consecutive S–H oxidative additions followed by the reductive release of a hydrogen molecule in complex **VII** produce complex **1** ***trans*** in a process that has to surmount a Gibbs energy barrier of 26.8 kcal mol^{-1}. The **XII** to **1** ***trans*** process is the rds for the formation of complex **1** ***trans***. This means that kinetically, the *cis* conformation is favored over the *trans* species by 0.9 kcal mol^{-1}. A final pathway to form complex **1** ***trans*** could be the isomerization of complex **VIII** to its *trans* conformation **XI**, that is, the rotation of the hydride by 90°. This transformation requires surpassing a barrier of 33.0 kcal mol^{-1} with respect to **I**, being the *trans* isomer 6.4 kcal mol^{-1} higher in energy. Therefore, this latter pathway can be ruled out. As a whole, our results show that formation of complex **1** ***cis*** is both thermodynamically and kinetically favored as compared to complex **1** ***trans*** formation. In both cases, the rds corresponds to the last step of the process that involves coordination of the phosphanylthiolato ligand and release of a H_2 molecule.

To further evaluate the preference for the *cis* isomer for complex **1**, its phenyl groups were substituted by either methyl or *tert*-butyl (*t*-Bu) groups, and then the *trans* isomer was found to be lower in Gibbs energy by 0.8 and 15.2 kcal mol^{-1}, respectively. These energy values reveal that highly sterically demanding groups like *t*-Bu impedes the formation of the *cis* conformation, and the comparison between methyl and phenyl substituents indicates a major preference of the *cis* for the latter substituent because of the π–π stacking between its aryl groups. The structural deformation due to the substituents on the phosphorous is translated into the increase of the P–Pt–P angle, by 0.4 and 12.0° with methyl and *t*-butyl groups, respectively (see Figure 3).

To explore the possibility to obtain the dinuclear complex [PtCl(μ-$SCH_2CH_2PPh_2$-κ^2*P,S*)]$_2$, similar to those observed for nickel[15] and palladium,[10a] the base-free reaction of [$PtCl_2$(COD)] (COD = 1,5-cyclooctadiene) with 1 equivalent of Hdppet in dichloromethane was performed, affording a quite insoluble material. According to the $^{31}P\{^1H\}$ NMR spectrum, this solid is formed mainly by two products in a 2/1 ratio. The minor component shows a singlet with a chemical displacement and a $^1J_{P-Pt}$ coupling constant similar to those observed for the bis-chelate complex **1**. The major constituent of the mixture also shows a singlet, but at higher fields and with larger $^1J_{P-Pt}$ coupling constant. Slow evaporation of the NMR solutions of this mixture produces a microcrystal (3 × 3 × 2 μm^3) which was studied by XRD. Crystal data for the structure obtained, complex **2**, are given in Table 1. Selected bond lengths and bond angles are listed in the caption of Figure 4.

The crystal structure reveals a sulfur-bridging edge-sharing cyclic trinuclear complex with square-planar coordination geometry around the platinum atoms (Figure 4). Related structures were found for aminoalkylthiolato, [PtBr(μ-$SCH_2CH_2NMe_2$-κ^2*N,S*)]$_3$,[22] phosphanylarylthiolato, [PtI(μ-SC_6H_4-2-PPh_2-κ^2*P,S*)]$_3$[23] and [PtI{μ-SC_6H_4-2-P(1,1′-biphenyl)-κ^2*P,S*}]$_3$,[24] and arsanylarylthiolato ligands, [PtI(μ-SC_6H_4-2-PAs_2-κ^2*As,S*)]$_3$,[25] but complex **2** is, to our knowledge, the first example with phosphanylalkylthiolato ligand.

The *cis*-Cl,P arrangement is in disagreement with the anti-symbiosis rule,[17] but the *cis*-S,S geometry is necessary to build

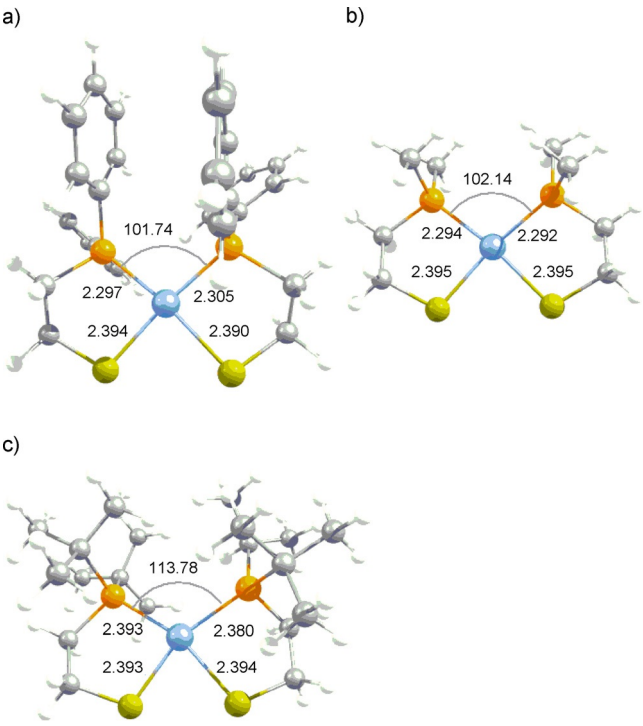

Figure 3. Optimized *cis* conformation of a) [Pt(dppet)$_2$] (**1**), b) [Pt(dmpet)$_2$], and c) [Pt(dtbpet)$_2$] (selected distances (Å) and angles (°)).

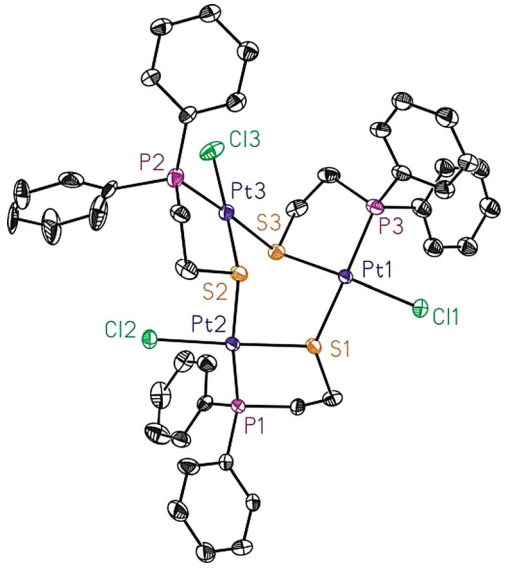

Figure 4. ORTEP figure (50%) of complex **2**, H atoms are omitted for the sake of clarity; selected distances (Å) and angles (°): Pt1–P3 2.246(2), Pt1–S3 2.283(2), Pt1–Cl1 2.340(2), Pt1–S1 2.3651(19), Pt2–P1 2.225(2), Pt2–S1 2.2648(19), Pt2–Cl2 2.3345(19), Pt2–S2 2.358(2), Pt3–P2 2.248(2), Pt3–S2 2.266(2), Pt3–Cl3 2.328(2), Pt3–S3 2.401(2), P3–Pt1–S3 87.67(8), S1–Pt1–S3 95.33(7), Pt1–S1–Pt2 109.66(8), P1–Pt2–S1 88.09(7), S1–Pt2–S2 83.73(7), Pt2–S2–Pt3 105.20(9), P2–Pt3–S2 86.98(8), S2–Pt3–S3 89.54(7), Pt1–S3–Pt3 111.25(8).

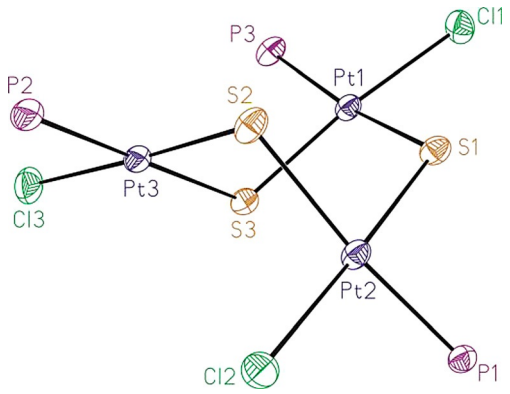

Figure 5. ORTEP figure (50%) of the Pt_3S_3 cycle with the platinum square-planar coordination sphere of complex **2**. Selected distances and angles are given in Figure 4.

the six-membered Pt_3S_3 cycle. This cycle adopts a skew-boat conformation (Figure 5) with each bridging sulfur atom showing one shorter and one longer Pt–S bond (Figure 4). Similar unsymmetrical bridging sulfurs were observed in related compounds.[23,24] The S–Pt–S angles are smaller than Pt–S–Pt ones because of the restriction imposed by the metal square-planar coordination. Two of the three five-membered chelate cycles adopt a δ conformation with both phenyl radicals of the PPh_2 group in a pseudo equatorial position. The third chelate cycle shows a λ conformation which locates one of the phenyl groups in axial position (Figure 6). On the face of the Pt_3S_3 cycle where this phenyl is placed, there is no other group that generates steric repulsions, resulting in the most favorable situation. Accordingly, the Pt–P and Pt–S distances are the shortest. The square-planar geometry around platinum is somewhat distorted with a chelate angle slightly reduced from the idealized value of 90°. Quite similar distortions from the idealized geometry are also observed in other platinum(II) complexes with chelated dppet ligands.[16,26] The intramolecular Pt–Pt distances are greater than 3.65 Å suggesting no metal–metal covalent interactions.

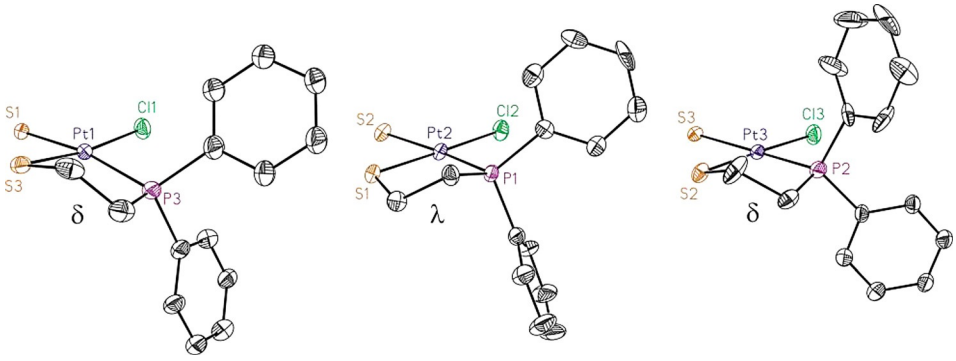

Figure 6. ORTEP figure (50%) of the Pt_3S_3 cycle with the platinum square-planar coordination sphere of complex **2**. Selected distances and angles are given in Figure 4.

Concerning the mechanism of the reaction, as we have observed in this work, the $^{31}P\{^1H\}$ NMR of the reaction mixture of one equivalent of the phosphanylarylthioarsine $Ph^2AsSC_6H_4$-2-PPh_2 with $[PtI_2(COD)]$ shows initially the existence of a mixture of the bis-chelate and a second complex with chemical displacement at lower frequencies and larger $^1J_{P-Pt}$ coupling constant. The second compound resulted to be the trinuclear $[PtI(\mu\text{-}SC_6H_4\text{-}2\text{-}PPh_2\text{-}\kappa^2P,S)]_3$.[23] This parallelism, and the crystal structure obtained, allow us to assign the major component of our reaction mixture to complex **2**. Regarding the reaction pathway, formation of the bis-chelate complex **1** has been postulated as the kinetically favored process, elapsing through a mononuclear intermediate (Scheme 2).[23] The subsequent reaction of **1** with the mononuclear intermediate and unconverted starting product (path A) can generate a trinuclear intermediate that should isomerize to the final thermodynamic product **2**.

This pathway is similar to that proposed for the formation of $[PtI(\mu\text{-}SC_6H_4\text{-}2\text{-}PPh_2\text{-}\kappa^2P,S)]_3$, in which the trinuclear intermediate was identified, and the kinetic product, the bis-chelate, is totally transformed into the ultimate trinuclear complex.[23] In present work, the trinuclear intermediate has not been detected, and no interconversion between complexes **1** and **2** was observed, pointing to a quick association of the mononuclear intermediate to give trinuclear complex **2** (pathway B in Scheme 2).

To understand the trinuclear structural preference for complex **2**, DFT calculations were carried for this complex and for the hypothetical binuclear intermediate $[PtCl(\mu\text{-}SCH_2CH_2PPh_2\text{-}\kappa^2P,S)]_2$, as well as for any moiety able to link complexes **1** and **2**. First, the structural results on complex **2** showed good agreement between the experimental and theoretical data. The standard deviation for the bond distances is 0.053 Å and that for the angles is 1.3°,[27,28] thus providing confidence in the reliability of the chosen method to reproduce geometries of the studied complexes. Furthermore, although there is the experimental insight that both mononuclear and trinuclear species are diamagnetic, we performed calculations for neutral closed-shell singlet ground-state structures, but we also checked how far was the lowest-lying excited triplet state. In all cases, the triplet state presented a higher energy (the difference between these two states for **1** is 31.9 kcal mol^{-1}), indicating that the singlet states are the most favored. This is in agreement with the sharp peaks in the NMR spectra.

Figures 7 and 8 map the paths B and A that drive $[PtCl_2(COD)]$ to **2** and **1**, respectively. The first step (**a** to **b** in Figure 7) involves the dissociation of the neutral COD ligand together with the coordination of a Hdppet ligand. This process releases 17.0 kcal mol^{-1}. This new square-planar intermediate **b** might be in competition with the cationic moiety where the leaving group was a chloride instead of the COD.

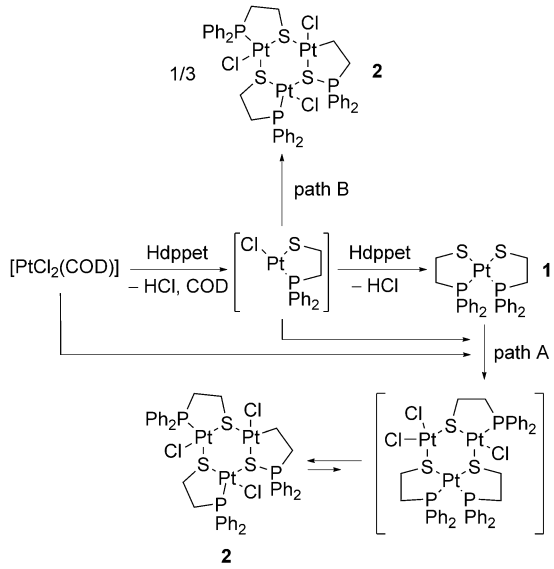

Scheme 2. Possible reaction pathways in the formation of complex **2**.

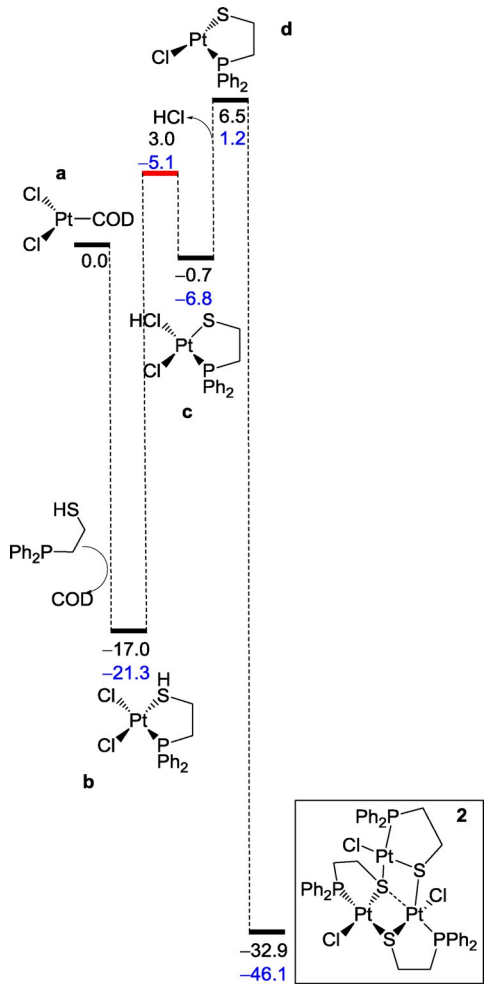

Figure 7. Reaction pathway of the conversion of $[PtCl_2(COD)]$ to complex **2** (red lines display the transition states, in blue is the corresponding profile with Hdmpet ligand, Gibbs energies relative to 3 $[PtCl_2(COD)]$ + 3 Hdmpet ligands (in kcal mol^{-1}).

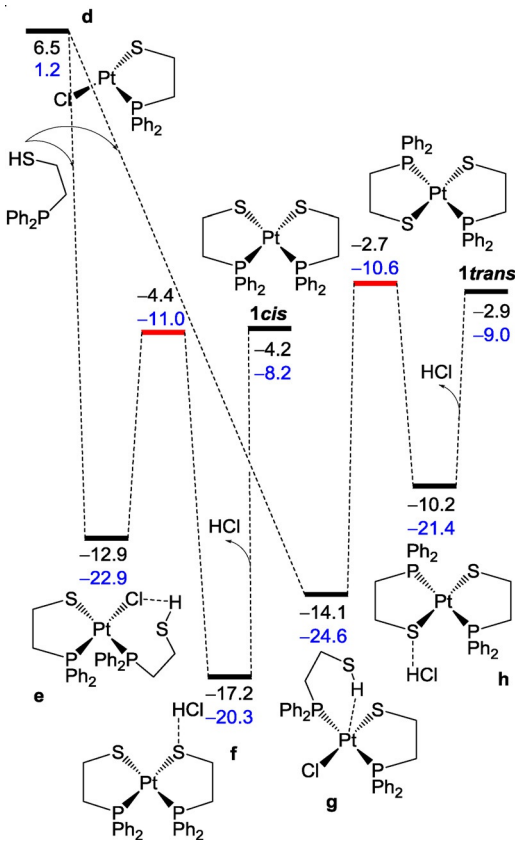

Figure 8. Reaction pathway of the conversion of intermediate **d** to complex **1** (red lines display the transition states, in blue is the corresponding profile with Hdmpet ligand, Gibbs energies relative to 3 $[PtCl_2(COD)]$ + 3 Hdmpet ligands (in kcal mol^{-1}).

Anyway chloride substitution is endergonic by 6.4 kcal mol^{-1}, and, therefore, COD release is much more favorable. The next proton transfer from the thiol group to the chloride and release of HCl molecule requires 23.5 kcal mol^{-1} and drives to a somewhat unstable intermediate **d** that trimerizes easily to complex **2**. The formation of this trinuclear complex from complex **d** is found to be barrierless and quite exergonic (39.4 kcal mol^{-1}). Thus this result shows that pathway B involves relatively low-energy-demanding steps, and it is thermodynamically favored.

Alternatively, instead of the trinuclear interaction, intermediate **d** can interact with a new Hddpet substrate molecule to yield complex **e** (Figure 8). This complex can easily be transformed into **f** after overcoming a barrier of 8.5 kcal mol^{-1}. Final release of an HCl molecule yields **1*cis*** complex in a process that is 21.4 kcal mol^{-1} endergonic. On the other hand, from species **d**, the *trans* conformation of **1** might be also feasible, overcoming a barrier 17.0 kcal mol^{-1}. Our results show that once complex **d** is generated, formation of **2** is kinetically and thermodynamically more favorable than obtaining any of the mononuclear species **1**. This result is in agreement with the principle of maximum hardness since the chemical hardness for complex **2** is 7.8 kcal mol^{-1} higher than that of complex **1*cis*.**

The dimerization was also faced, instead of the trimerization. Although the process to get the dimeric structures, including

either two chloride or sulfur bridges is barrierless, thermodynamically it is 30.2 kcal mol^{-1} less favorable than the formation of the trinuclear structure. On the other hand, the other trinuclear structure proposed as an intermediate in path A (Scheme 2) was also investigated, but located to be 6.6 kcal mol^{-1} higher in energy than **2**. Despite its rather high stability, its formation requires the formation of complex **1** first, which is ruled out according to the mechanism proposed in Figure 8.

The substitution of the phenyl groups by methyl or *tert*-butyl groups on the phosphorous atoms did not change any qualitative trend, and quantitatively all barriers were nearly identical. Thermodinamically, the energy released with respect to the precursor [$PtCl_2$(COD)] in the formation of **2** is higher when the phenyl groups in the phosphines are substituted by methyl (13.2 kcal mol^{-1}) or *tert*-butyl (8.7 kcal mol^{-1}) groups. This confirms that the nature of phosphine substituents is not determining the feasibility of the formation of trinuclear species.

Conclusions

The transition metal complexes of heterotopic phosphanylthiolato ligands are important for their use in many interesting reactions. In this work, bis-chelate complex [Pt($SCH_2CH_2PPh_2$,κ^2*P,S*)$_2$] (**1**) has been obtained in good yields by direct base-free substitution reaction of the corresponding thiol with K_2PtCl_4 or by oxidative addition of the thiol to $Pt(PPh_3)_4$. The XRD studies of this complex **1** shows a *cis*-P,P arrangement in agreement with the antisymbiosis rule. Density functional theory (DFT) calculations on **1** indicate that the *cis* geometry is preferred over the *trans* one for both thermodynamic and kinetic reasons. The rate determining step for the formation of complex **1** is the final step, which involves an oxidative addition of the S–H bond of a phosphanylthiol ligand into the Pt center and the reductive release of a hydrogen molecule. Direct base-free reaction of [$PtCl_2$(COD)] with one equivalent of the thiol produces the trinuclear complex [PtCl(μ-$SCH_2CH_2PPh_2$-κ^2*P,S*)]$_3$ (**2**) with square-planar coordination geometry around the platinum atoms and a Pt_3S_3 cycle in skew-boat conformation. Our DFT calculations show that formation of the trinuclear structure occurs through ClPt(dppet) complex **d**. Once this rather unstable intermediate is formed, the formation of the trinuclear structure is a barrierless and quite exergonic process. On the contrary, formation of the mononuclear and dinuclear species involves non-negligible energy barriers and leads to thermodynamically less stable products.

Experimental Section

Synthesis

General remarks: The complexes were synthesized using standard Schlenk techniques under N_2 atmosphere. The solvents were dried by standard methods and distilled and deoxygenated before use. The C, H, and S analyses were carried out using a Carlo–Erba microanalyser (Lakewood, USA). ^{1}H NMR spectra were recorded at 200 MHz on a Bruker DPX-200 spectrometer (Billerica, USA). Peak positions are relative to tetramethylsilane (TMS) as internal reference. ^{31}P{^{1}H} NMR spectra were recorded on the same instrument operating at 81.0 MHz. Chemical shifts are relative to external 85% H_3PO_4, and downfield values are reported as positive.

[Pt{$SCH_2CH_2PPh_2$-κ^2*P,S*}$_2$] (1). *Method 1*: Hdppet (30 mg, 0.12 mmol) in MeOH (2 mL) was added to a solution of K_2PtCl_4 (24.7 mg, 0.06 mmol) in deionized H_2O (3 mL). The mixture was allowed to react for 30 min at rt, the solvent is evaporated in vacuo down to 0.5 mL, and Et_2O (1 mL) is slowly added to precipitate an intense yellow microcrystalline solid. The product is separated by filtration, washed with Et_2O, and dried under a current of N_2 yielding complex **1** (24 mg, 92%). *Method 2*: neat Hdppet (112 mg, 0.44 mmol) was added to a solution of $Pt(PPh_3)_4$ (285 mg, 0.22 mmol) in CH_2Cl_2 (8 mL). The mixture is allowed to react for 30 min at rt, and hexane (1 mL) is slowly added to precipitate **1** (105 mg, 70%). Completely dry complex **1** is stable in air, slightly soluble in CH_2Cl_2 and insoluble in $CHCl_3$, EtOH, MeOH, toluene, Et_2O, and hexane. ^{1}H NMR (200 MHz, CD_2Cl_2, TMS): δ = 2.52 (m, 4H, aliphatics), 7–8 ppm (m, 10H, aromatics). ^{31}P{^{1}H} NMR (81 MHz, CD_2Cl_2, H_3PO_4): δ = 61.70 ppm (s, $^1J_{P-Pt}$ = 2810.9 Hz). The low solubility of **1** precluded the observation of a good-quality ^{13}C NMR spectrum. Anal. calcd for $C_{28}H_{28}P_2PtS_2$ (685,7): C 49.05, H 4.12, S 9.35; found C 49.29, H 4.30, S 9.65.

[PtCl(μ-$SCH_2CH_2PPh_2$-κ^2*P,S*)]$_3$ (2): neat Hdppet (123 mg, 0.50 mmol) was added to a solution of [$PtCl_2$(COD)] (236.5 mg, 0.50 mmol) in CH_2Cl_2 (8 mL). The mixture was allowed to react for 1 h at rt, the solvent was evaporated in vacuo down to 3 mL, and Et_2O (5 mL) was slowly added to give a yellow precipitate. The product was separated by filtration, washed with Et_2O, and dried under a current of N_2, yielding a solid (189.7 mg) practically insoluble in CH_2Cl_2, and insoluble in $CHCl_3$, Et_2O, and hexane. The low solubility of this solid precluded the observation of good-quality NMR spectra. ^{31}P{^{1}H} NMR (81 MHz, CD_2Cl_2, H_3PO_4): major product δ = 45.27 ppm (s, $^1J_{P-Pt}$ = ca. 3343 Hz), minor product δ = 62.18 ppm (s, $^1J_{P-Pt}$ = ca. 2771 Hz).

X-ray crystal structure determination

Yellow crystals of **1** were obtained by slow evaporation of CH_2Cl_2/hexane solutions at rt. Yellow crystals of **2** were obtained by slow evaporation of a CH_2Cl_2 solution. Measured crystals were prepared under inert conditions immersed in perfluoropolyether as protecting oil for manipulation. Crystal data are presented in Table 1, and selected distances and angles in the captions of Figure 1 and 4.

Data collection: Crystal structure determinations for **1** and **2** were carried out using a Siemens P4 diffractometer (Munich, Germany) equipped with an SMART 1000 CCD area detector, a MAC Science Co. rotating anode with MoKα radiation, a graphite monochromator, and a Siemens low-temperature device (T = −120 °C). Full-sphere data collection was used with ω and ϕ scans. *Programs used*: Data collection SMART,[29] data reduction SAINT,[30] and absorption correction SADABS.[31]

Structure Solution and Refinement: Crystal structure solution was achieved using direct methods as implemented in SHELXTL[32] and visualized using the program XP. Missing atoms were subsequently located from difference Fourier synthesis and added to the atom list. Least-squares refinement on F^2 using all measured intensities was carried out using the program SHELX-93. All nonhydrogen atoms were refined including anisotropic displacement parameters.

Comments on the structures: Compound **1** crystallizes with a half molecule in the asymmetric unit showing *C2* symmetry. Com-

pound **2** crystallizes with one molecule in the asymmetric unit. Four of the benzenes rest linked to the phosphorous atoms are disordered in two orientations with an approximate ratio of 60:40. Although the triclinic crystal used for the structure determination of **2** was of extremely small dimensions ($3\times3\times2\ \mu m^3$), an excellent dataset could be collected.

Computational methods

All the DFT calculations were performed at the generalized gradient approximation (GGA) level with the Gaussian09 set of programs,[33] using the M06 functional of Truhlar.[34] The electronic configuration of the molecular systems was described with the standard split-valence basis set with a polarization function of Ahlrichs and co-workers for H, C, N, P, S, and Cl (SVP keyword in Gaussian).[35] For Pt we used the quasi-relativistic Stuttgart/Dresden effective core potential, with an associated valence basis set (standard SDD keywords in Gaussian09).[36] The geometry optimizations were carried out without symmetry constraints, and the characterization of the stationary points was performed by analytical frequency calculations. These frequencies were used to calculated unscaled zero-point energies (ZPEs) as well as thermal corrections and entropy effects at 298 K and 1 atm by using the standard statistical-mechanics relationships for an ideal gas. Energies were obtained via single point calculations on the M06-optimized geometries with triple zeta valence plus polarization (TZVP keyword in Gaussian) using the M06 functional as well.[30] In these single-point energy calculations, H, C, N, P, S, and Cl were described using the TZVP basis set, while for Pt, the SDD basis set was employed. On top of the M06/TZVP/M06/SVP energies, we added the ZPEs, thermal corrections obtained at the M06/SVP level. In addition, to calculate the reported Gibbs energies, we included solvent effects of a CH_2Cl_2 solution estimated with the polarizable continuous solvation model PCM implemented in Gaussian09.[37] The chemical potential is a measure of the tendency of the electrons to escape from the system. It is calculated from the partial derivative of the electronic energy with respect to the total number of electrons. The hardness, η, is a measure of the resistance of a chemical species to change its electronic configuration, and it is defined as the second-order partial derivative of the total electronic energy with respect to the total number of electrons. Using a finite difference approximation and the Koopmans' theorem, one obtains the expressions we have used for the calculation of the chemical potential and the hardness:

$$\mu = \frac{\varepsilon_{LUMO} + \varepsilon_{HOMO}}{2}, \quad (1)$$

$$\eta = \frac{\varepsilon_{LUMO} - \varepsilon_{HOMO}}{2}, \quad (2)$$

where ε_{LUMO} and ε_{HOMO} are the energies of the low unoccupied molecular orbital (LUMO) and the high occupied molecular orbital (HOMO), respectively.

Acknowledgements

A. Polo thanks the Spanish Dirección General de Enseñanza Superior e Investigación Científica (DGESIC) for financial support (project BQU2002-04070-C02-01). A. Poater thanks the Spanish Ministerio de Economía y Competitividad (MINECO) for a Ramón y Cajal contract (RYC-2009-05226) and the European Commission for a Career Integration Grant (CIG09-GA-2011-293900). M. S. thanks the European Union for a Fonds Européen de Développement Régional (FEDER) fund (UNGI10-4E-801), the Generalitat de Catalunya for project 2014SGR931 and the Institució Catalana de Recerca i Estudis Avançats (ICREA) Academia 2014 prize, and MINECO through project CTQ2014-54306-P.

Keywords: bis-chelate complexes · density functional calculations · P,S ligands · platinum · trinuclear complexes

[1] For reviews on the use of heterotopic phosphorus-sulfur donor ligands in catalytic processes, see: a) D. K. Dutta, B. Deb, *Coord. Chem. Rev.* **2011**, *255*, 1686 – 1712; b) J. R. Dilworth, N. Wheatley, *Coord. Chem. Rev.* **2000**, *199*, 89 – 158.

[2] J. S. Kim, J. H. Reibenspies, M. Y. Darensbourg, *J. Am. Chem. Soc.* **1996**, *118*, 4115 – 4423.

[3] H. Kuniyasu, F. Yamashita, T. Hirai, J.-H. Ye, S.-I. Fujiwara, N. Kambe, *Organometallics* **2006**, *25*, 566 – 570.

[4] a) M. Yuki, Y. Miyake, Y. Nishibayashi, *Organometallics* **2010**, *29*, 5994 – 6001; b) W.-C. Chu, C.-C. Wu, H.-F. Hsu, *Inorg. Chem.* **2006**, *45*, 3164 – 3166.

[5] L.-P. He, M. Hong, B.-X. Li, J.-Y. Liu, Y.-S. Li, *Polymer* **2010**, *51*, 4336 – 4339.

[6] N. Brugat, A. Polo, A. Álvarez-Larena, J. F. Piniella, J. Real, *Inorg. Chem.* **1999**, *38*, 4829 – 4837.

[7] a) R. J. Angelici, *Organometallics* **2001**, *20*, 1259 – 1275; b) D. A. Vicic, W. D. Jones, *J. Am. Chem. Soc.* **1999**, *121*, 7606 – 7617.

[8] a) S. Ye, F. Neese, A. Ozarowski, D. Smirnov, J. Krzystek, J. Telser, J.-H. Liao, C.-H. Hung, W.-C. Chu, Y.-F. Tsai, R.-C. Wang, K.-Y. Chen, H.-F. Hsu, *Inorg. Chem.* **2010**, *49*, 977 – 988; b) T.-W. Chiou, W.-F. Liaw, *Inorg. Chem.* **2008**, *47*, 7908 – 7913; c) C.-M. Lee, Y.-L. Chuang, C.-Y. Chiang, G.-H. Lee, W.-F. Liaw, *Inorg. Chem.* **2006**, *45*, 10895 – 10904; d) T. Ohkubo, H. Sakashita, T. Sakuma, M. Kainosho, M. Sekiguchi, K. Morikawa, *J. Am. Chem. Soc.* **1994**, *116*, 6035 – 6036; e) L. C. Myers, M. P. Terranova, A. E. Ferentz, G. Wagner, G. L. Verdine, *Science* **1993**, *261*, 1164 – 1167.

[9] P. W. N. M. Van Leeuwen, P. C. J. Kamer, J. N. H. Reek, P. Dierkes, *Chem. Rev.* **2000**, *100*, 2741 – 2769.

[10] a) N. Brugat, J. Duran, A. Polo, J. Real, A. Álvarez-Larena, J. F. Piniella, *Tetrahedron: Asymmetry* **2002**, *13*, 569 – 577; b) J. Duran, N. Brugat, A. Polo, J. Real, X. Fontrodona, J. Benet-Buchholz, *Organometallics* **2003**, *22*, 3432 – 3438; c) J. Duran, A. Polo, J. Real, J. Benet-Buchholz, A. Poater, M. Solà, *Eur. J. Inorg. Chem.* **2003**, 4147 – 4151.

[11] a) A. Dervisi, R. L. Jenkins, K. M. A. Malik, M. B. Hursthouse, S. Coles, *Dalton Trans.* **2003**, 1133 – 1142; b) A. Dervisi, D. Koursarou, L.-L. Ooi, P. N. Horton, M. B. Hursthouse, *Dalton Trans.* **2006**, 5717 – 5724.

[12] Y.-M. Hsiao, S. S. Chojnacki, P. Hinton, J. H. Reibenspies, M. Y. Darensbourg, *Organometallics* **1993**, *12*, 870 – 875.

[13] P. H. Leung, J. W. L. Martin, S. B. Wild, *Inorg. Chem.* **1986**, *25*, 3396 – 3400.

[14] M. Kita, T. Yamamoto, K. Kashiwabara, J. Fujita, *Bull. Chem. Soc. Jpn.* **1992**, *65*, 2272 – 2274.

[15] T. Gerdau, W. Klein, R. Kramolowsky, *Cryst. Struct. Commun.* **1982**, *11*, 1663 – 1669.

[16] P. V. Rao, S. Bhaduri, J. Jiang, D. Hong, R. H. Holm, *J. Am. Chem. Soc.* **2005**, *127*, 1933 – 1945.

[17] R. G. Pearson, *Inorg. Chem.* **1973**, *12*, 712 – 713.

[18] J. N. Harvey, K. M. Heslop, A. G. Orpen, P. G. Pringle, *Chem. Commun.* **2003**, 278 – 279.

[19] a) R. G. Parr, L. von Szentpaly, S. Liu, *J. Am. Chem. Soc.* **1999**, *121*, 1922 – 1924; b) P. Geerlings, F. De Proft, W. Langenaeker, *Chem. Rev.* **2003**, *103*, 1793 – 1873; c) R. G. Parr, W. Yang, *Density Functional Theory of Atoms and Molecules*, Oxford University Press, New York, **1989**; d) R. G. Parr, R. A. Donnelly, M. Levy, W. E. Palke, *J. Chem. Phys.* **1978**, *68*, 3801 – 3807; e) R. G. Parr, R. G. Pearson, *J. Am. Chem. Soc.* **1983**, *105*, 7512 – 7516; f) T. Koopmans, *Physica* **1934**, *1*, 104 – 113.

[20] a) R. G. Pearson, *J. Chem. Educ.* **1987**, *64*, 561 – 562; b) R. G. Pearson, *Chemical Hardness, Applications from Molecules to Solids*, Wiley-VCH, Oxford, **1997**.

[21] a) A. J. Bridgeman, N. Harris, N. A. Young, *Chem. Commun.* **2000**, 1241 – 1242; b) A. J. Bridgeman, *J. Chem. Soc. Dalton Trans.* **1996**, 2601 – 2607; c) A. Poater, *J. Phys. Chem. A* **2009**, *113*, 9030 – 9040; d) A. Poater, A. G. Saliner, R. Carbó-Dorca, J. Poater, M. Solà, L. Cavallo, A. P. Worth, *J. Comput. Chem.* **2009**, *30*, 275 – 284; e) A. Poater, A. G. Saliner, M. Solà, L. Cavallo, A. P. Worth, *Expert Opin. Drug Delivery* **2010**, *7*, 295 – 305.

[22] M. Capdevila, W. Clegg, P. Gonzalez-Duarte, I. Mira, *J. Chem. Soc. Dalton Trans.* **1992**, 173 – 181.

[23] I. Sárosi, A. Hildebrand, P. Lönnecke, L. Silaghi-Dumitrescu, E. Hey-Hawkins, *Dalton Trans.* **2012**, *41*, 5326 – 5333.

[24] A. Hildebrand, I. Sárosi, P. Lönnecke, L. Silaghi-Dumitrescu, M. B. Sárosi, I. Silaghi-Dumitrescu, E. Hey-Hawkins, *Dalton Trans.* **2012**, *41*, 7729 – 7736.

[25] A. Hildebrand, I. Sárosi, P. Lönnecke, L. Silaghi-Dumitrescu, M. B. Sárosi, I. Silaghi-Dumitrescu, E. Hey-Hawkins, *Inorg. Chem.* **2012**, *51*, 7125 – 7133.

[26] J. Duran, R. Juanola, A. Polo, J. Real, J. Benet-Buchholz, M. Solà, A. Poater, *Unpublished data.*.

[27] The chosen bond distances and angles used for the comparison of the theoretical and experimental data are collected in Table S2 in the Supporting Information.

[28] a) A. Poater, S. Moradell, E. Pinilla, J. Poater, M. Solà, M. A. Martínez, A. Llobet, *Dalton Trans.* **2006**, 1188 – 1196; b) M. Costas, X. Ribas, A. Poater, J. M. López-Valbuena, R. Xifra, A. Company, M. Duran, M. Solà, A. Llobet, M. Corbella, M. A. Usón, J. Mahía, X. Solans, X. Shan, J. Benet-Buchholz, *Inorg. Chem.* **2006**, *45*, 3569 – 3581; c) J. Mola, M. Rodríguez, I. Romero, A. Llobet, T. Parella, A. Poater, M. Duran, M. Solà, J. Benet-Buchholz, *Inorg. Chem.* **2006**, *45*, 10520 – 10529.

[29] Data collection with SMART version 5.060 Bruker-AXS, Bruker AXS Inc., Madison, WI, **1999**.

[30] Data reduction with Bruker SAINT V6.02 Bruker AXS, Bruker AXS Inc., Madison, WI, **1999**.

[31] a) SADABS: V2001 Bruker, Bruker AXS Inc., Madison, WI, **2001**; b) R. H. Blessing, *Acta Crystallogr. Sect. A* **1995**, *51*, 33 – 38.

[32] SHELXTL version V6.14, G. M. Sheldrick, *Acta Crystallogr. Sect. A* **2008**, *64*, 112 – 122.

[33] Gaussian 09, Revision D.01, M. J. Frisch, G. W. Trucks, H. B. Schlegel, G. E. Scuseria, M. A. Robb, J. R. Cheeseman, G. Scalmani, V. Barone, B. Mennucci, G. A. Petersson, H. Nakatsuji, M. Caricato, X. Li, H. P. Hratchian, A. F. Izmaylov, J. Bloino, G. Zheng, J. L. Sonnenberg, M. Hada, M. Ehara, K. Toyota, R. Fukuda, J. Hasegawa, M. Ishida, T. Nakajima, Y. Honda, O. Kitao, H. Nakai, T. Vreven, J. A. Montgomery, Jr., J. E. Peralta, F. Ogliaro, M. Bearpark, J. J. Heyd, E. Brothers, K. N. Kudin, V. N. Staroverov, R. Kobayashi, J. Normand, K. Raghavachari, A. Rendell, J. C. Burant, S. S. Iyengar, J. Tomasi, M. Cossi, N. Rega, J. M. Millam, M. Klene, J. E. Knox, J. B. Cross, V. Bakken, C. Adamo, J. Jaramillo, R. Gomperts, R. E. Stratmann, O. Yazyev, A. J. Austin, R. Cammi, C. Pomelli, J. W. Ochterski, R. L. Martin, K. Morokuma, V. G. Zakrzewski, G. A. Voth, P. Salvador, J. J. Dannenberg, S. Dapprich, A. D. Daniels, Ö. Farkas, J. B. Foresman, J. V. Ortiz, J. Cioslowski, D. J. Fox, Gaussian, Inc., Wallingford CT, **2009**.

[34] Y. Zhao, D. G. Truhlar, *Theor. Chem. Acc.* **2008**, *120*, 215 – 241.

[35] A. Schäfer, H. Horn, R. Ahlrichs, *J. Chem. Phys.* **1992**, *97*, 2571 – 2577.

[36] a) U. Häussermann, M. Dolg, H. Stoll, H. Preuss, P. Schwerdtfeger, R. M. Pitzer, *Mol. Phys.* **1993**, *78*, 1211 – 1224; b) W. Küchle, M. Dolg, H. Stoll, H. Preuss, *J. Chem. Phys.* **1994**, *100*, 7535 – 7542; c) T. Leininger, A. Nicklass, H. Stoll, M. Dolg, P. Schwerdtfeger, *J. Chem. Phys.* **1996**, *105*, 1052 – 1059.

[37] a) V. Barone, M. Cossi, *J. Phys. Chem. A* **1998**, *102*, 1995 – 2001; b) J. Tomasi, M. Persico, *Chem. Rev.* **1994**, *94*, 2027 – 2094.

Received: May 19, 2015
Published online on July 30, 2015

